International Journal of Scientific Engineering and Applied Science (IJSEAS) - Volume-1, Issue-8,November 2015
ISSN: 2395-3470
www.ijseas.com

Geochemical characteristics of goethite-bearing deposits in the Dakhla – Kharga oases, Western Desert, Egypt

Sherif Farouk[1], Mohamoud El-Rahmany[2], Hatem El-Desoky[2], Ahmed Khalil[3], Wael Fahmy[2]

1. Exploration Department, Egyptian Petroleum Research Institute, Nasr City, 11727, Egypt
2. Department of Geology, Faculty of Science, Al-Azhar University, Cairo, Egypt
3. Department of Geology, National Research Center, Cairo, Egypt

Abstract: Detailed field observations and geochemical studies were carried out to assess the origin and depositional environment of widely distributed lateritic and limonite ore covered floor of the Dakhla-Kharga oases. It ranges in thickness from 0.5 to 8 m, overlying different Upper Cretaceous rocks, particularly the red clay of the Campanian Quseir Formation located in the Dakhla Oasis, or the Cenomanian Sabaya Formation in the Kharga Oasis. The lateritic iron ores in the present study consists mainly of massive yellow goethite-rich beds with a high accumulation of Fe_2O_3 ranging from 82 - 55 %, while the Fe/Mn ratios ranges from 4515 to 25. The presences of high Fe/Mn ratio with a wide range of variation indicated that the sources of the iron deposits is from the discharge of iron-rich Nubian Aquifer water controlled largely by localized fractures which formed spring mounds deposited during the Pleistocene age. These mounds which were exposed to subaerial weathering that resulted in the formation of lateritic limonite ore during arid climatic periods. The widely distribution of limonite iron ore in topographic areas that are less complicated and have high content of Fe_2O_3, shed some light on the importance of extracting the limonite ore, which is nearly absent in North Africa.

Keywords: Goethite, iron, paleosols, Dakhla, Kharga, Western Desert, Egypt.

1. Introduction

Iron ores are recorded in few localities in Egypt including, Bahariya, Aswan, central part of Eastern Desert and West-central Sinai. The current study marks to add some information about a new resource of lateritic limonite ore in the Dakhla-Kharga oases. Laterites are highly weathered materials rich in iron oxides, alumina or both. These deposits are rich in economic limonite ore which nearly missing in the North Africa including Egypt (Fig. 1). Furthermore, no any previous work was done on these iron ores in the Dakhla-Kharga oases except **Adelsberger and Smith (2010)**. They recognized iron-rich deposits in spring mounds and as archaeological sites where Paleolithic materials have been recovered. These spring mound sediments were deposited in a shallow vegetated wetland formed by the discharge of iron-rich Nubian Aquifer water, along the southern margin of the Oasis. The aim of this work is to investigate a more details about the distribution and physical criteria of lateritic limonite paleosol from filed observation, mineralogy, geochemistry and genesis in the Dakhla-Kharga oases.

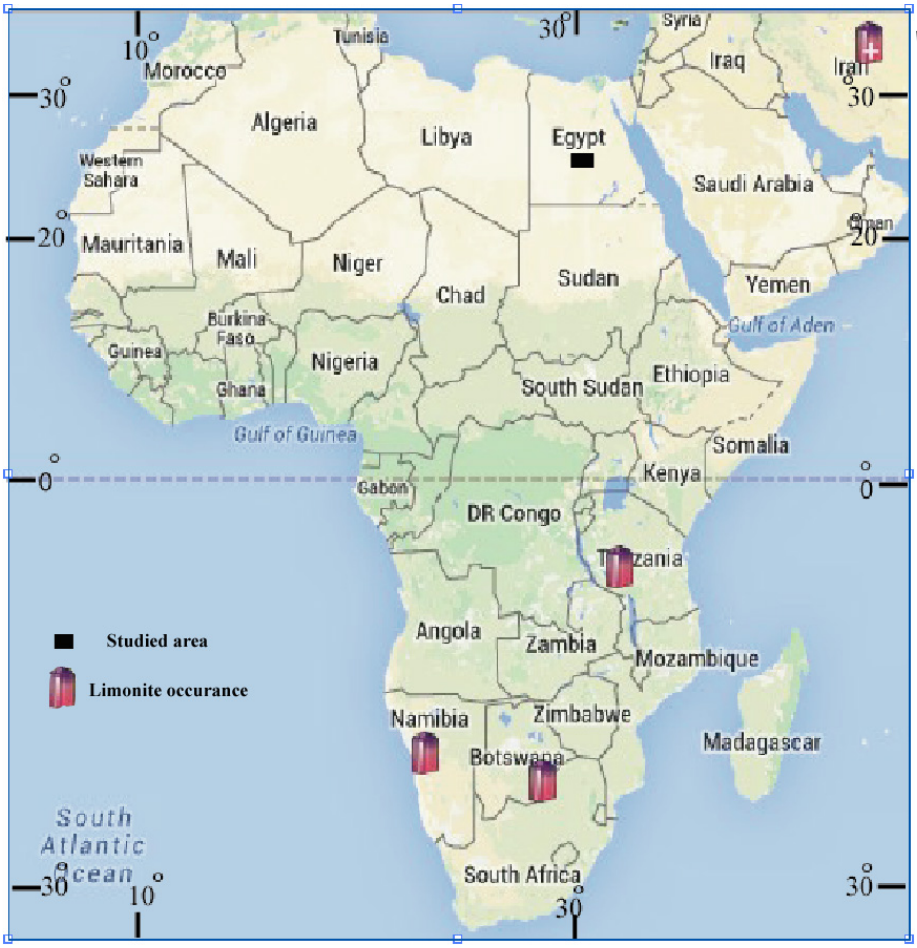

Fig.1. Distribution of the limonite iron ores in Africa and Middle East (source from Google Earth).

2. Geologic setting

The Dakhla – Kharga oases represented a major part of the central Western Desert of Egypt, according to geomorphologic classification. It can be considered a fifth order mega depression (**Embabi, 2004**). It is a part of the stable shelf which generally includes the horizontal strata forming the Western Desert plateau (**Said, 1962**). The stratigraphic succession in the Dakhla –Kharga oases is classified into the following sequence:

Lower siliciclastic sequences (Late Jurassic –Lower /Middle Campanian), which is comprised mainly of sandstone and few fine siliciclastics that are previously known as Nubian Sandstone, which subdivided into six rock units from oldest to youngest as follows: Six Hills, Abu Ballas, Sabaya, Maghrabi, Taref and Quseir formations. These siliciclastics sequences are widely exposed in Dakhla Oasis, along the length of the foot of the piedmont and widely forms its cultivated floor. Upper siliciclastics /carbonate sequence (Upper Campanian – Lower Eocene), is widely distributed in the base of the escarpment faces of the Dakhla Oasis. It has a general E-W direction, and bounds the depression of the Dakhla – Kharga oases on its northern side, reaching about 450-550m above sea level (a.s.l). These sequences are composed of phosphate, shale, marl and claystone with limestone beds. It was deposited in a shallow to deep marine environment. This succession is subdivided into four rock units from oldest to youngest as follows: Duwi, Dakhla, Tarawan, and their latter facies changes the Kurkur and Garra formations. The latest–Paleocene-Early Eocene Esna Shale and Thebes Formations have been recorded along the northern escarpment of the Kharga

Oasis. The depression floor of the Dakhla-Kharga oases is mainly covered by Quaternary deposits comprising alluvial, playa, internal sabkha, aeolian, and paleosol deposits.

The Quaternary paleosols represented by goethite rich deposits ranges from 0.5 to 8 m thickness, and covers a wide aerial distribution as a remnant above the red clay, which considered as a bed marker and the lower member of the Albian to Early Cenomanian Sabaya Formation or Campanian Quseir Formation in the Dakhla- Kharga depression floor. The goethite rich deposits in the Dakhla –Kharga oases were mainly distributed in the depression floor at about 125 – 250 m above sea level (Figs. 2-3).

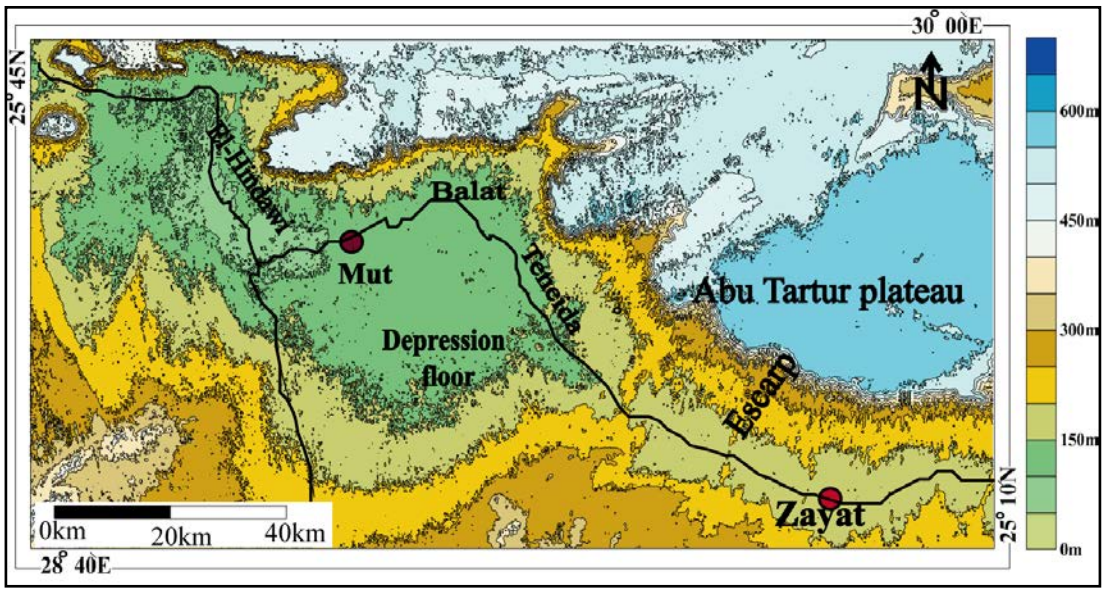

Fig. 2. Topographic map of the Dakhla-Kharga oases showing the studied area, depression, settlements, and topography (obtained from the DEM of the SRTM-03).

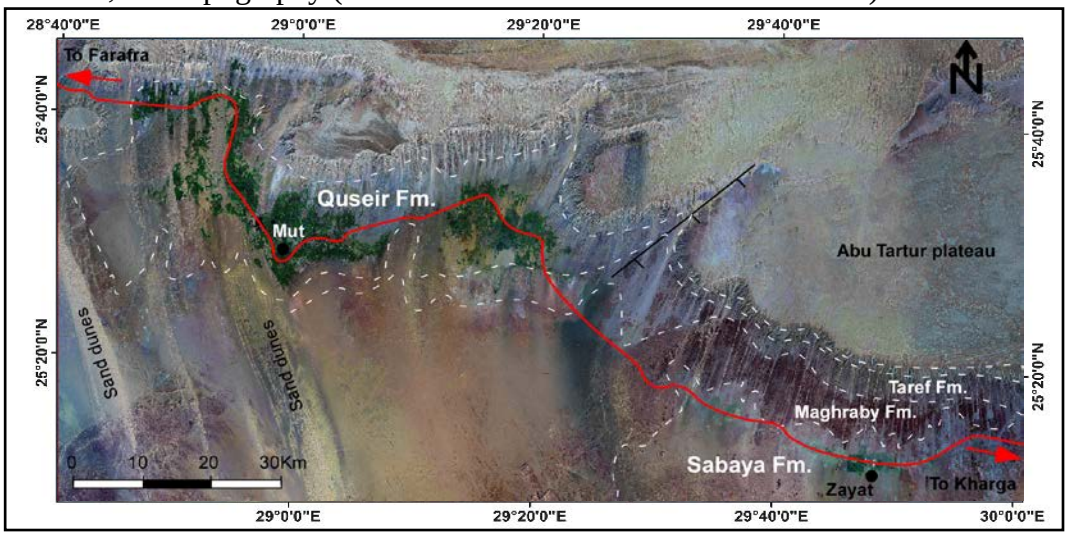

Fig. 3. Satellite image showing the distribution of the Sabaya and Quseir formations at the Dakhla-Kharga district

3. Materials and analytical methods

The present work is based on field observations and laboratory analysis of the limonite deposited covering the floor of the Dakhla-Kharga depression. Eleven representative samples were collected from two sections (Fig.3), nine samples at Mut area in Dakhla Oasis (Mut section) and three samples at Zayat area in Kharga Oasis (Zayat section). A Sample powders was analyzed for their mineralogical composition using a X-ray powder diffraction (XRD) technique. Chemical analysis of the selected samples by X-ray fluorescence was carried out for determination of major oxides and trace elements at the National Research Center (NRC) laboratories. Polished thin sections were prepared and investigated using a conventional optical microscope. Qualitative analysis was performed on hematite, goethite and magnetite using a SEM with (EDS Link AN 10000 System). Standard petrographic thin sections were prepared and examined for analysis of microfabrics; identify the iron ore minerals, mineralogical composition, and texture.

4. Results

4.1. Major oxides distribution

Data of XRF analyses of eleven selected samples of the Mut and Zayat areas are shown in (Tables 1 & 2). The Fe_2O_3 in the red clay reach to 7.28%, which strongly increases upward between 63.69% - 71.02%. In the Zayat section, the Fe_2O_3 of the Sabaya Formation, which covered the depression floor, reaches to 0.61% and it sharply increases to ranging between 41and 79%. Fe_2O_3 shows strong negative correlation with the SiO_2, Al_2O_3, TiO_2, K_2O and P_2O_5contents (r= -0.9,-0.8, -0.6, -0.7 and -0.7 respectively).It has strong positive correlation with Na_2O (r= 0.7).

SiO_2 contents in the analyzed samples of Mut area ranges between 8.74 and 21.16wt % with an average 18.59% except the red clays bed of Quseir Formation which SiO_2 content reaches up to 42.54%. In Zayat samples, it ranges between 4.02 and 24.02.6% except sample 33 which the SiO_2 content reaches to 82.6%.SiO_2 content has strong positive correlation with TiO_2,CaO and SiO_3 (r= 0.8, 0.8 and 0.7 respectively) while it has strong negative correlation with Fe_2O_3,$Na_2O$and L.O.I (r=-.09, -0.6 and -0.5 respectively). The average content of Al_2O_3 in the studied samples of Mut area is 4.85% with an exceptional high Al_2O_3 contents in the claystone sample no 2 (14.27%) while the average Al_2O_3 content in Zayat samples are (4.0%). Al_2O_3 has strong negative correlation with Fe_2O_3(r=-0.6%).The average contents of TiO_2, CaO, MgO, Na_2O, K_2O, and P_2O_5 are relatively low in all analyzed samples (averages of 0.5, 0.8, 0.8, 0.5, 0.97, and 0.05 wt.%, respectively.

4.2. Mineralogy

In the Mut section (Fig.4), X-ray diffraction reflects from base to top, the red clays of the Quseir Formation are composed mainly of quartz (36 -50.5%), halite (47%). Illite (16.5%) and dolomite (36%), the colorations of the red clay result of groundwater discharge from the Nubian Aquifer that acts as pigment. At the contact between the red clays and yellowish iron deposited, there are sandstone beds rich in quartz (36.7%) and vesuvianite (36.2%). The yellowish iron deposited are composed mainly of goethite with increase upward ranging from 25.7% to 60%.and quartz only (ranging from 40 to 74.2%).

At Zayat section (Fig.5), the iron-rich deposited occurs above the ferruginous sandstone of the Sabaya Formation (sample 33). It is mainly composed of goethite (7.6%), quartz (79.1%) and kaolinite (13.1%). The iron ore in Zayat section is composed mainly of goethite (ranging from 61 to 67.1%) and quartz only (ranging from 32.8 to 39%) similar to the iron deposited in Mut section. XRD analysis (Fig.6) indicated that goethite mineral (FeO

n(OH) is the main iron ore in the studied samples and it can identified in the XRD pattern by its characteristic peak at 4.19 Å where it reaches to about 67% in some samples (Table.3). Goethite an iron oxyhydroxides occurs with typically massive, silty-size. It could be formed as a primary mineral in hydrothermal deposits (**Hassaan *et al.*, 2015**). Magnetite minerals are appears as little amount in some samples, which reaches to about 13.1% in the red clay bed of Quseir Formation, detrital quartz are probably concentrated with the lateritic iron ore by wind action.

Table 1. Geochemical data of iron samples of the studied area (Major oxides wt. %)

S.No. / Oxides	2	4	5	6	8	11	7	12	33	35	40
	+	△					▶		◆	▼	
	Mut								Zayat		
	Claystone	Ferruginous sandstone							Ironstone		
SiO2	42.54	21.16	18.95	17.95	15.32	9.74	14.3	8.74	82.6	4.02	24.02
TiO2	0.89	0.42	0.50	0.59	0.40	0.36	0.43	0.26	0.83	0.29	0.80
Al_2O_3	14.27	3.29	3.51	3.60	3.55	3.61	3.56	3.41	3.88	0.58	7.42
Fe_2O_3	7.28	61.67	63.69	64.05	65.15	70.02	66.8	71.02	0.61	79.41	56.76
MnO	0.23	0.16	0.10	0.10	0.48	0.66	0.38	0.54	0.01	0.02	0.01
MgO	5.03	0.34	0.54	0.53	0.49	0.42	0.48	0.41	0.42	0.42	0.25
CaO	3.91	0.59	0.30	0.30	0.20	0.14	0.22	0.13	2.89	0.12	0.39
Na_2O	0.35	0.53	0.67	0.66	0.55	0.41	0.54	0.40	0.28	0.65	0.57
K_2O	3.88	0.72	0.81	0.81	0.75	0.61	0.71	0.51	1.02	0.03	0.83
P_2O_5	0.17	0.03	0.04	0.03	0.05	0.05	0.04	0.04	0.05	0.01	0.01
SO_3	0.19	1.13	0.78	0.65	1.42	1.87	1.32	1.89	6.22	0.36	0.33
Cl	2.19	0.51	0.68	0.60	0.65	0.47	0.57	0.43	0.11	0.19	0.39
L.O.F	18.8	8.50	9.08	9.28	10.01	11.18	10.1	11.27	0.78	13.79	7.43
Total	99.94	99.06	99.63	99.13	99.04	99.53	99.5	99.05	99.7	99.9	99.2

Table 2. Geochemical data of iron samples of the studied area (ppm).

S.No. / Trace elements	2	4	5	6	8	11	7	12	33	35	40
	Mut								Zayat		
V	0	163	159	375	64	21	38	39	0	482	100
Sr	93	342	330	50	55	66	22	123	42	88	13
Pb	0	126	129	199	145	154	152	135	0	183	91
Nb	21	51	52	14	22	20	16	16	0	19	62
Co	0	286	319	732	142	339	193	634	22	126	337
Zr	163	1125	1207	718	459	30	87	144	526	363	1118
Zn	80	450	402	836	121	129	357	562	0	49	763
Cs	0	474	538	357	346	344	357	270	0	344	491
Re	0	132	134	161	138	166	198	122	0	165	121
Au	0	151	150	173	94	138	93	178	0	173	141
Rh	0	169	163	150	148	131	164	132	0	136	171
CIA	64	60	61	62	66	72	66	73	48	33	77

Table 3. Relative abundance of iron ore and others minerals for the Sabaya and Quseir Formations in Dakhla – Kharga District.

Area	Sample number	Goethite %	Magnetite %	Quartz %	Illite %	Halite %	Kaolinite %	Dolomite %	Vesuvianite %
Mut	2	UN	**13.1**	**50.5**	UN	UN	UN	**36**	UN
	2\	UN	UN	**36**	**16.5**	**47**	UN	UN	UN
	4	UN	UN	**36.7**	UN	UN	UN	UN	**36.2**
	5	**25.7**	UN	**74.2**	UN	UN	UN	UN	UN
	7	**30**	UN	**60**	UN	UN	UN	UN	UN
	8	**47**	UN	**53**	UN	UN	UN	UN	UN
	11	**60**	UN	**40**	UN	UN	UN	UN	UN
Zayat	33	**7.6**	UN	**79.1**	UN	UN	**13.1**	UN	UN
	35	**67.1**	UN	**32.8**	UN	UN	UN	UN	UN
	40	**61**	UN	**39**	UN	UN	UN	UN	UN

Table 4. Showing Fe/Mn ratio for the studied ironstone samples.

S.No. / Chemical com,	2	4	5	6	8	11	7	12	33	35	40
	+	△					▶		◆	▼	
	Mut								Zayat		
	Claystone	Ferruginous sandstone							Ironstone		
Fe	**5**	**43**	**45**	**45**	**46**	**49**	**47**	**50**	**0**	**56**	**40**
Mn	**0.18**	**0.12**	**0.08**	**0.08**	**0.37**	**0.51**	**0.3**	**0.4**	**0.01**	**0.0**	**0.0**
Fe/Mn	**29**	**356**	**560**	**575**	**123**	**96**	**159**	**118**	**55**	**4131**	**4515**
Si	**19.9**	**9.9**	**8.9**	**8.4**	**7.2**	**4.5**	**6.70**	**4.08**	**38.6**	**1.88**	**11.22**
Al	**7.6**	**1.7**	**1.9**	**1.9**	**1.9**	**1.9**	**1.88**	**1.80**	**2.1**	**0.31**	**3.93**
Ti	**0.5**	**0.2**	**0.3**	**0.4**	**0.2**	**0.2**	**0.26**	**0.16**	**0.5**	**0.17**	**0.48**
CIA	**64**	**60**	**61**	**62**	**66**	**72**	**66**	**73**	**48**	**33**	**77**

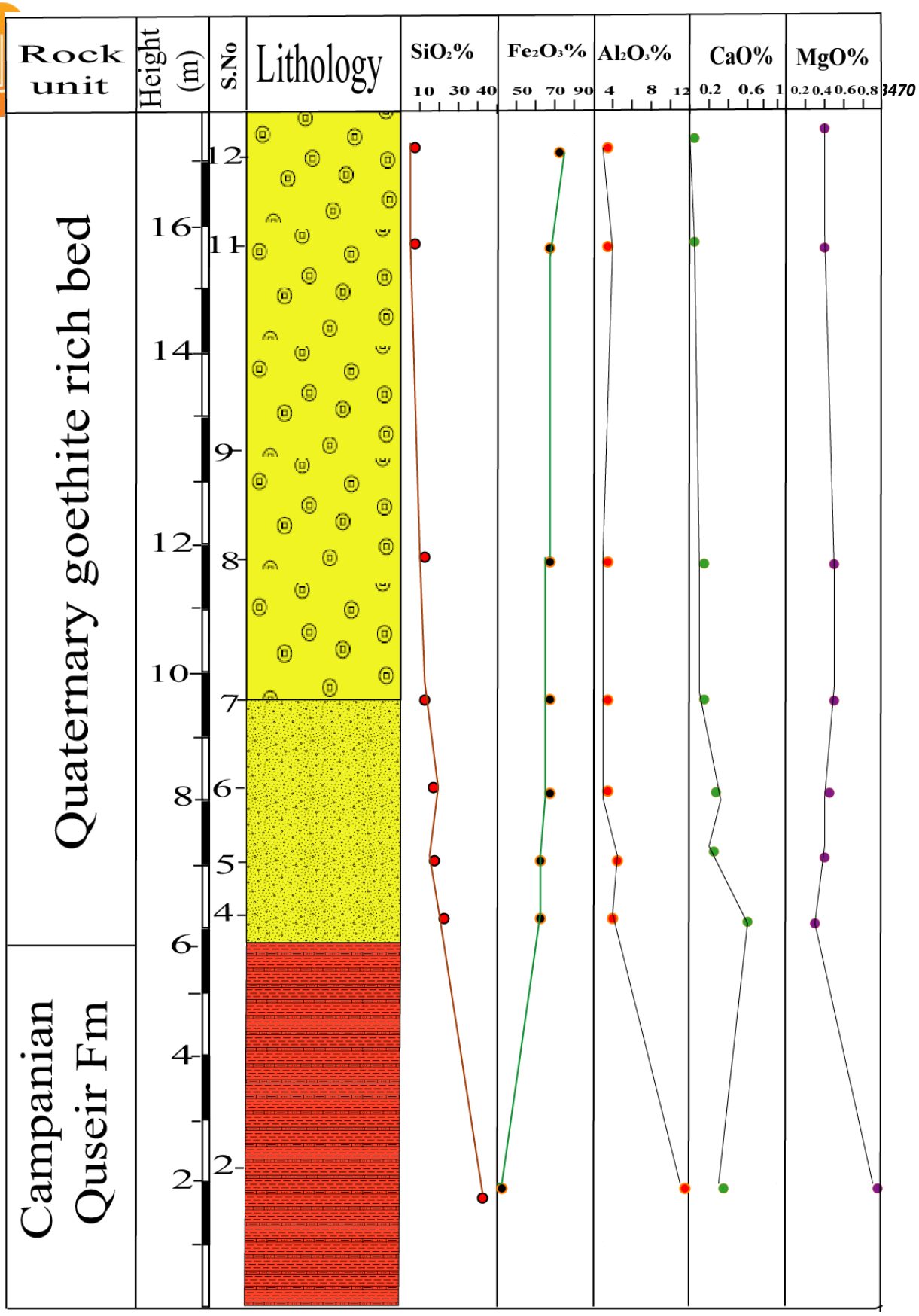

Fig. 4. Lithostratigraphic columnar section with sample positions and major oxides distribution at Mut area. For symbol key see Fig. 5.

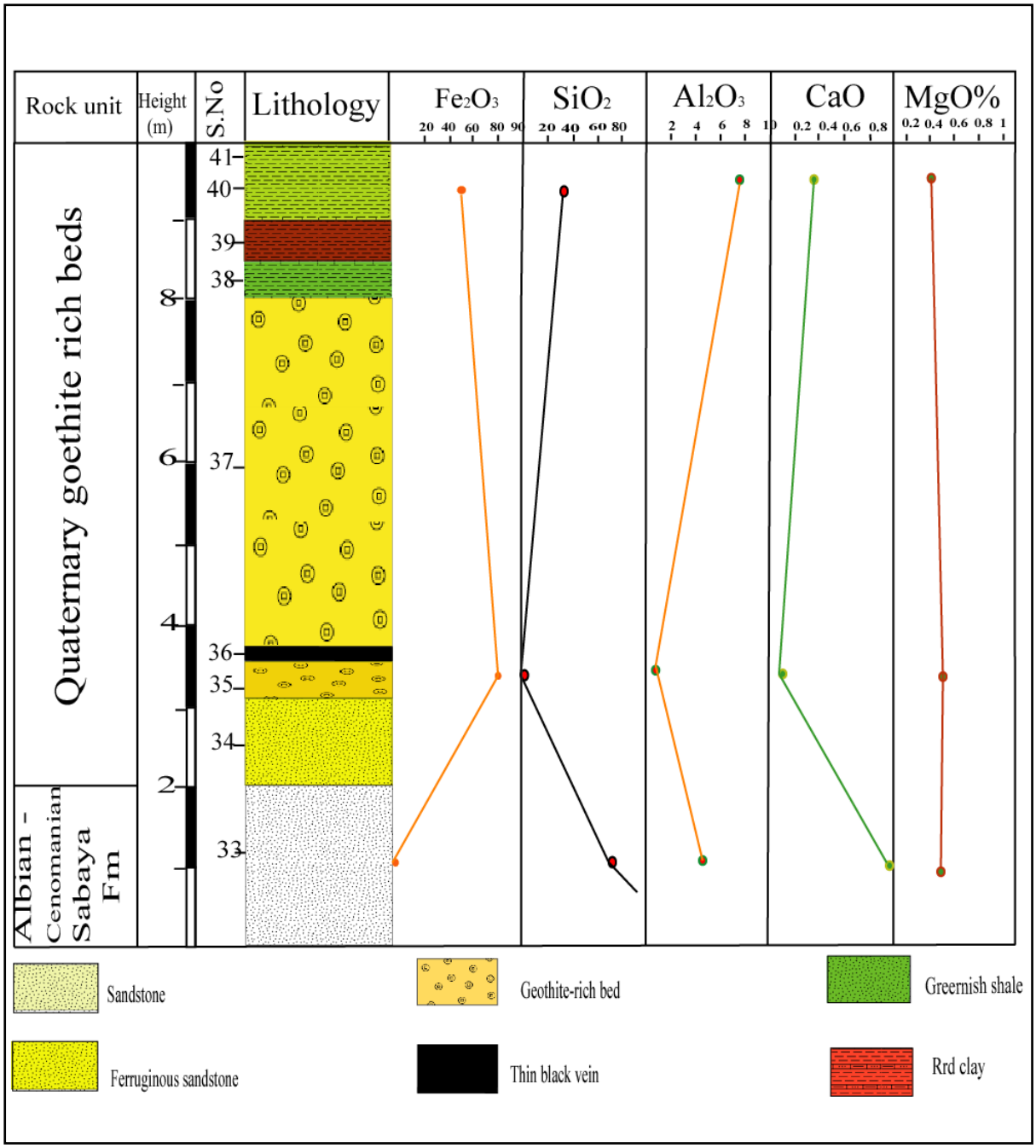

Fig. 5. Lithostratigraphic columnar section with sample positions and major oxides distribution at Zayat area.

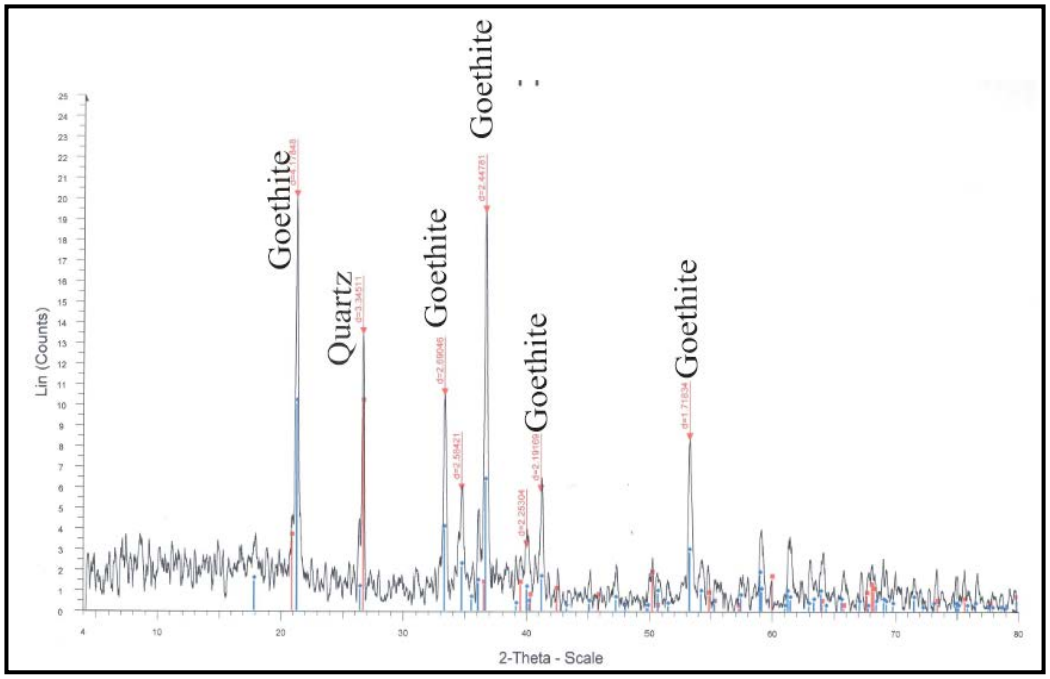

Fig.6. X-ray diffraction pattern for representative sample of iron from the Dakhla Oasis with key diffraction peaks indicated for quartz and goethite minerals.

4-3 Classification

The Geochemical classification of the analyzed 11 iron samples is shown by **Herron's diagram (1988)** which indicate that most of the studied samples fall in the Fe- shale and Fe-sand except the red claystone of Quseir Vegetated Shale (sample 2), which fall in shale field and sandstone of Sabaya Formation (sample 33), which fall in subarkose field (Fig.7). Depending on SiO_2- Fe_2O_3-Al_2O_3 ternary diagram of **Dury (1969**; Fig.8**),** show that the data pointed fall in the field of Fe- laterite and ferruginous –siliceous duricrusts except sample 33 which fall in the silicretes field.

4.4. Environment of Deposition

The geochemical distribution of certain major and minor elements may provide direct information on the depositional environment of the host sediments. It is emphasized, however, that it may be misleading to attempt to use the absolute abundance values of a single element as an indicator of the environment (**Degens *et al.*, 1957**). The relation between $LogK_2O/Al_2O_3$ and MgO/Al_2O_3 was used by **Roaldest (1978)** to differentiate between marine and non-marine clay. Application of this relation on the studied iron samples (Fig.9) revealed that all samples fall within non- marine environment except sample 2 which related to the brick red claystone of Quseir Formation fall in marine field.

4.5. Source of iron

The high Fe/Mn ratios (>10) fall within wide range of variations between 29 and 4515, while the relationships between (MnO/TiO_2)-(Fe_2O_3/TiO_2) ratio reflects that the iron-rich deposits formed mainly from early rapid hydrothermal solutions (**Crerar *et al.*, 1982; Adachi *et al.*, 1986;** Figs.10 & 11). Therefore, we describe the source of limonite deposited as spring mounds in the sense of **Adelsberger and Smith (2007).**

This interpretation is supported also by the field observations, where many trends of indurated ferruginous sandstone are recorded in the Taref Formation (Fig.12). It is structurally controlled largely by localized fractures and indicates that permeability was the controlling factor in the distribution of iron in these beds. In addition to, the iron-rich deposited especially in the Upper Cretaceous clastic rocks at the Dakhla-Kharga oases are the result of groundwater discharge from the Nubian Aquifer (**Brookes, 1993**) that act as pigment. **Salem *et al.* (2013)** uses the satellite remote sensing tools and some geochemical analysis recorded a paleosols iron-rich deposited between the Abu Aggag and Timsah Formations in the Kurkur landform of Lake Naser basin, Western Desert, Egypt. We consider in the present study, the source of this iron-rich paleosols coming from the same source, where the Fe/Mn ratio of Lake Naser basin areas indicate that are hydrothermal origin where it is ranging between 60 and 867 in Lake Naser basin, 128 to 225 in Abu Aggag Formation, 197 to 2220 in Timsah Formation and from 248 to 3378 in Abu Simble area. **Tanner and Khalifa (2009)** depart from the interpretation of **Catuneanu *et al.* (2006)** in attributing the iron accumulation solely to the processes of pedogenesis and laterization in the Lower Cenomanian Bahariya Formation, Bahariya Oasis of the Western Desert. They consider it more likely that the accumulation of the iron was largely the result of groundwater activity during early diagenesis and that the distribution was controlled primarily by sediment permeability.

Limonite deposited with silt-size in the present study area occurs mainly above undulating boundary and is widely distributed along an irregular unconformable surface that reflects a subaerial exposure during a period of emergence landscape stability and oxidative weathering (Fig.13). This interpretation is support by the chemical index of alteration (CIA) which defined as CIA = $\{Al_2O_3 / (Al_2O_3+CaO+Na_2O+K_2O)\}*100$ has been established as a general indicator of the degree of weathering in any provenance region **(Nesbitt and Young, 1982**). In the studied samples, the CIA content is more than 60 which indicate intensive chemical weathering in the source area with the exception of the some ironstone samples of Zayat area (33 and 35) which contains CIA value (48, 33 respectively; Table 4). **Goldberg and Humayun (2010)** used the CIA (molar) versus K_2O/Na_2O and Al_2O_3 as a paleo-humidity indicator. The relationships between the K_2O/Na_2O versus CIA (molar) for the studied iron are reflects an arid environment except two samples from the red clay (sample 2) in Mut area and ironstone (sample 35) in Zayat area falls in filed tropical environment (Fig. 14).

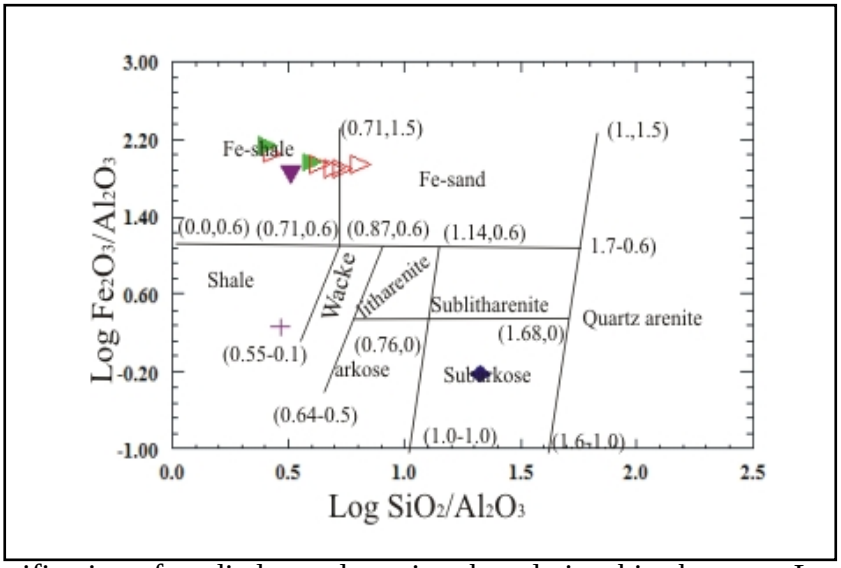

Fig. 7. Classification of studied samples using the relationships between Log SiO_2/Al_2O_3-Log Fe_2O_3/Al_2O_3 on the binary diagram (**Herron, 1988**), which falls in the ferrigenous sandstone and shale filed. For symbol key see Table 1.

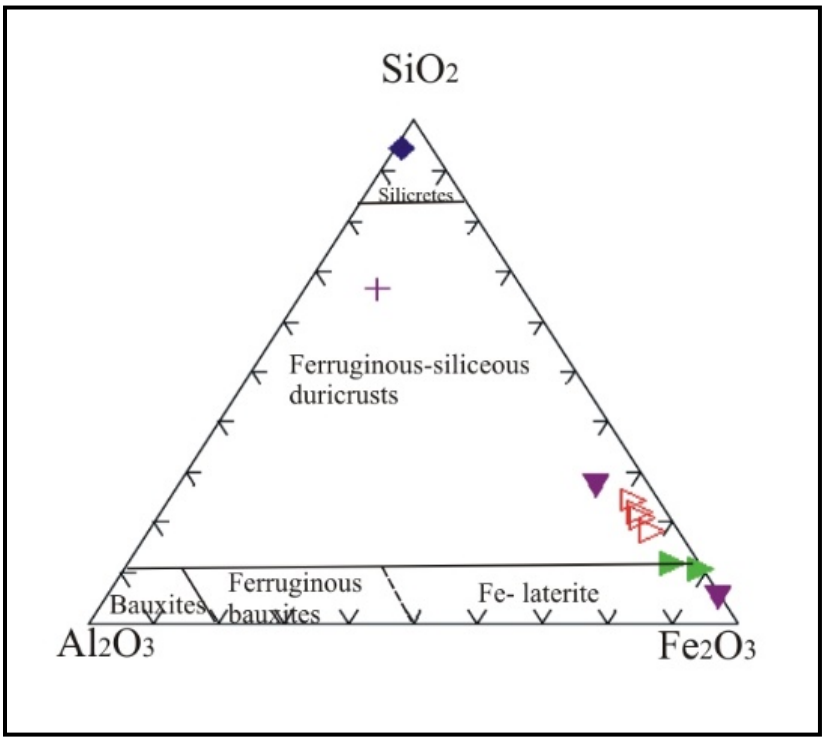

Fig. 8. Relationship between SiO_2- Al_2O_3-Fe_2O_3 on the ternary digram (**Dury, 1969**) for analyzed iron ore in the Dakhla-Kharga district. For symbol key see Table 1.

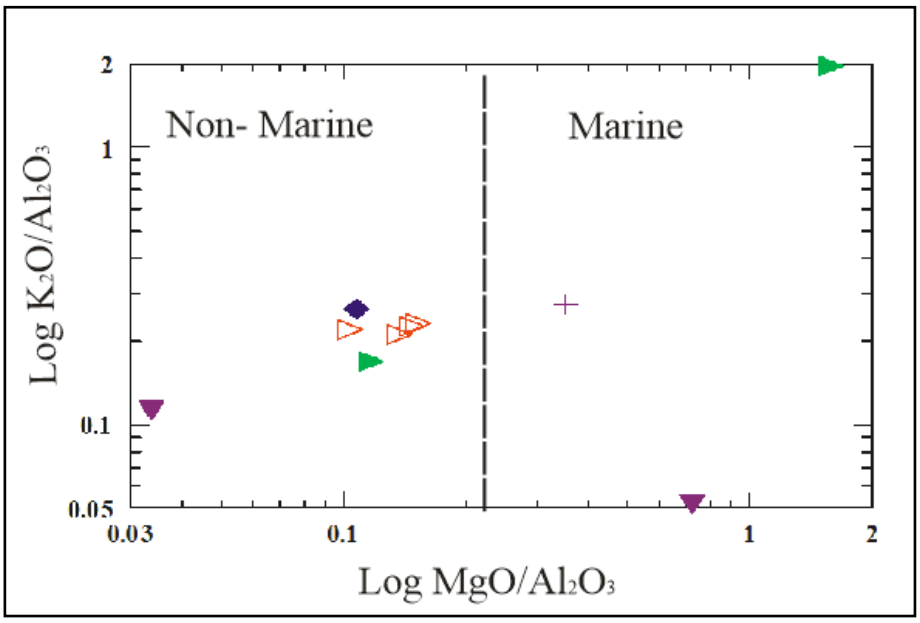

Fig. 9. Depositional environment of the studied samples based on the relation between log MgO/Al_2O_3 and log K_2O/Al_2O_3 (**Roaldest, 1978**). For symbols key see Table 1.

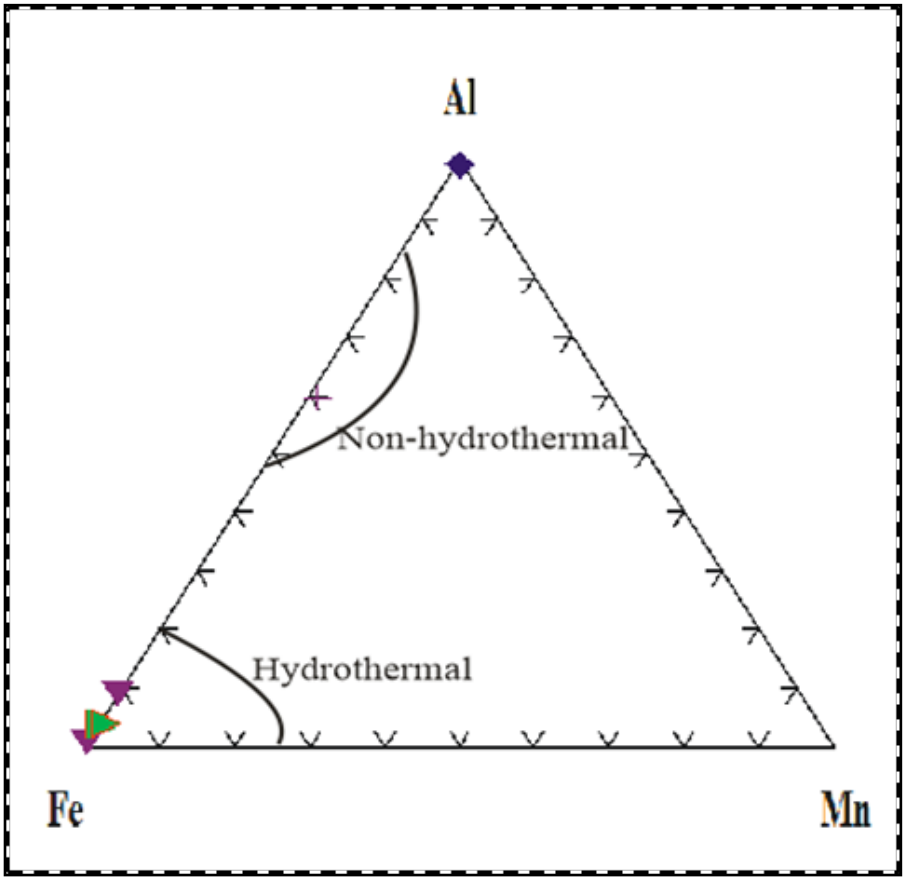

Fig.10. Relationship between Al-Fe-Mn on the ternary diagram (**Adachi *et al.*, 1986)** for analyzed iron ore in the Dakhla-Kharga district. For symbol key see Table 1.

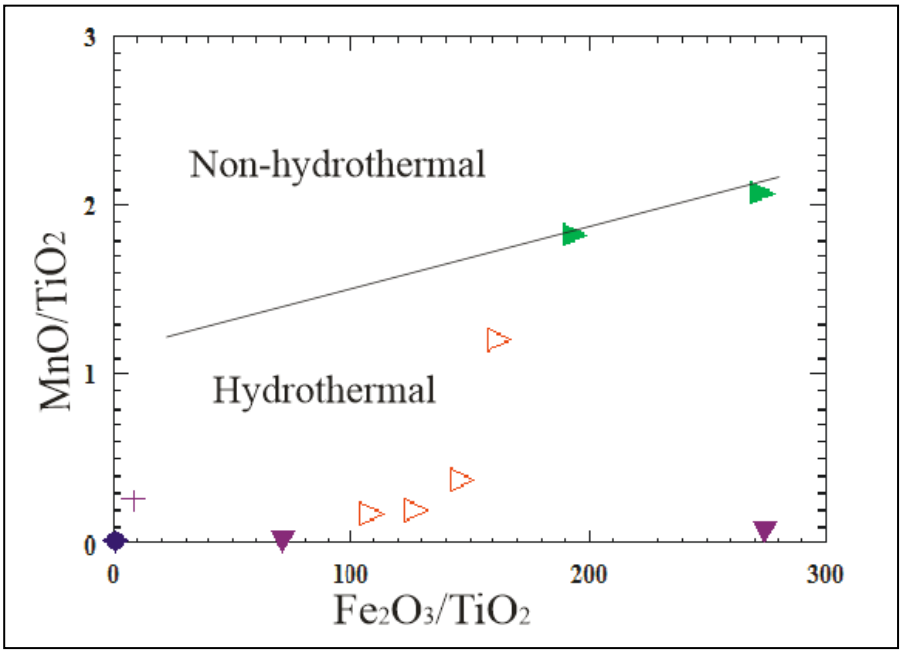

Fig.11. Plot of MnO/TiO_2 versus Fe_2O_3/TiO_2 on the binary diagram (**Adachi *et al.*, 1986)** for analyzed iron ore in the Dakhla-Kharga district.

Fig.12. Indurated ferruginous sandstone trends controlled largely by localized fractures which recorded in the Taref Formation. The outcrop is 200 m in length.

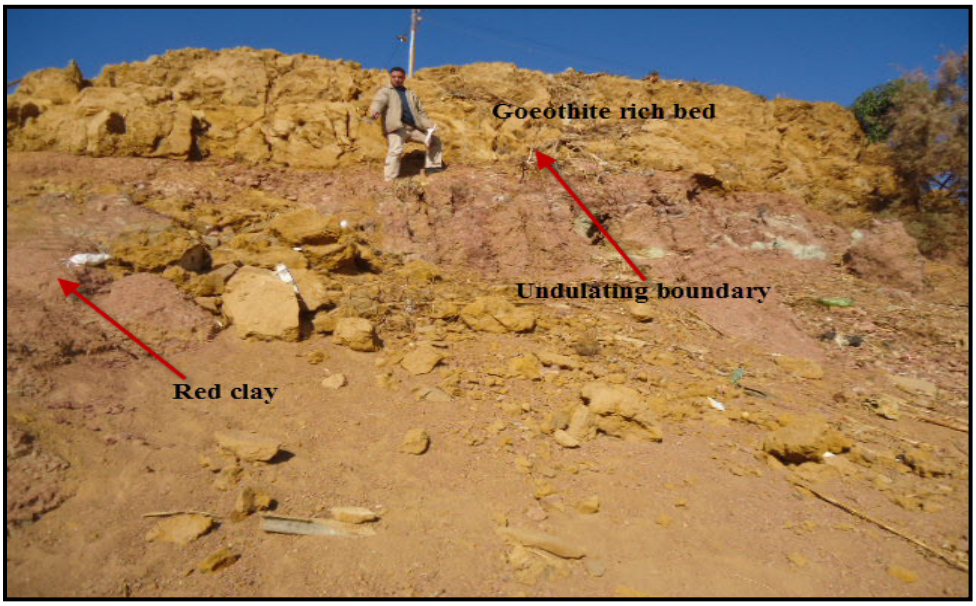

Fig.13. Filed photographic showing the ferralitic paleosol (red beds) lies below the undulating boundary with the goethite-rich bed indicating a period of emergence and oxidative weathering.

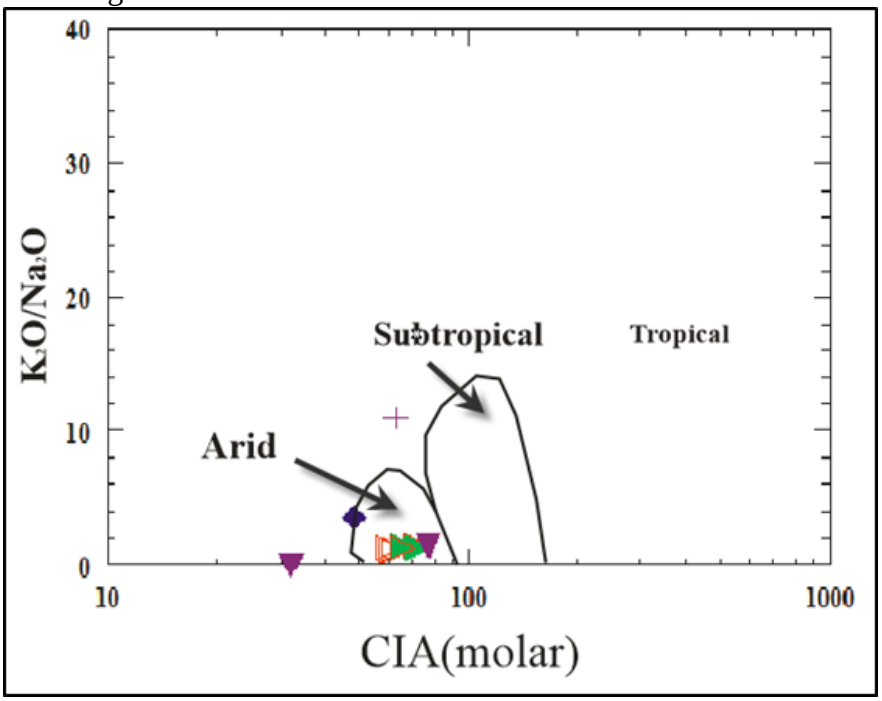

Fig.14. Plot of the CIA (molar) versus K_2O/Na_2O **(Goldberg and Humayun, 2010)** for analyzed iron ore in the Dakhla-Kharga district, which falls mainly in the arid conditions.

5. Conclusions

There is a wide distribution of non-marine limonite deposited with an average thickness ranging from 0.5 to 8 m of Quaternary age are observed. These deposits are recorded as remnants overlying the sandstone of Sabaya Formation or red clay of the Quseir

Formation, which cover the floor of the Dakhla – Kharga depression. Geochemistry data revealed strong negative correlation of Fe_2O_3 with silica and alumina thus indicating there is no iron silicate phase as well as alumina contribution from iron oxide minerals in the form of solid solution is insignificant. The studied iron samples contains an average content of P_2O_5 of 0.04% with a high accumulation of Fe_2O_3 ranging from 82 - 55 % reflects Bessemer grades. The studied samples are classified as Fe-laterite and ferruginous –siliceous duricrusts. These indicate that sediments exposed to the deep weathering process. The mineralogical data suggest the main iron ore in the studied area is goethite mineral with little amount of hematite and magnetite which suggest the hydrothermal origin of the studied samples. In the study area, the limonite deposited formed originally from rapid hydrothermal solutions by the discharge of iron-rich Nubian Aquifer water. The Fe/Mn ratios (>10) have a wide range of variations between 29 and 4515 reflects intensive chemical weathering under mainly arid and tropical environments.

References

Adachi, M.K., Yamamto, K., Sugisaki, R., 1986. Hydrothermal cherts and associated siliceous rocks from northern Pacific: their geological significance as indication of ocean ridge activity. Sed. Geol., 47,125-148.

Adelsberger, K.A., Smith, J.R., 2010. Paleolandscape and paleoenvironmental interpretation of spring-deposited sediments in Dakhleh Oasis, Western Desert of Egypt. Jorn. Catena, 83, 7–22.

Brookes, I.A., 1993. Late Pleistocene basinal sediments, Dakhla Oasis region. Egypt, Aoninterglacial pluvial: Geoscient Red NE Africa, Berlin, Ger, p.627-633. Egypt. Acad. Sci. 16, 61-70.

Catuneanu, O., Khalifa, M.A., Wanas, H.A., 2006. Sequence stratigraphy of the Lower Cenomanian Bahariya Formation, Bahariya Oasis, Western Desert, Egypt. Sedimentary Geology, 190, 121–137.

Crerar, D.A., Navson, J., Cuyr, M.S., Wrrlnlurs, L., Fercrnson, M.D., 1982. Manganiferous cherts of the Franciscan assemblage. General geology, ancient and modern analogues, and implications for hydrothermal convection at oceanic spreading centers. Econ. Geol. 77, P519-540.

Degens, E.T., Williams, E.G., Keith, M.L., 1957. Environmental studies of Carboniferous sediments. Part I: Geochemical criteria for differentiating marine and fresh water shales. AAPG Bull., 41, P 2427-2455.

Dury, G.H., 1969. Perspectives on geomorphic processes. Washington: Association of American Geographers, 1969. 56.

Embabi, N.A., 2004. The Geomorphology of Egypt: land form as and evolution. Vol.1: the Nile Valley and Western Desert. Egypt. Geographic society, special Pub. Rocks in Egypt. Annual Meeting .Geol. Soc. Egypt, Cairo, June 12.

Goldberg, K., Humayun, M., 2010. The applicability of the Chemical Index of Alteration as a paleoclimatic indicator: An example from the Permian of the Paraná Basin, Brazil. Paleogeography, **293**; P175–183.

Hassaan, M.A., El-Afandy, El-Desoky, H.M., Asran, H.M., Soliman, O.A., 2015. Studies on ferrugination in Gabal Agib ring complex, South Eastern Desert, Egypt. Nuclear Sciences Scientific Journal,. 4, 1-18.

Herron, M.M., 1988. Geochemical classification of terrigenous sands and shales from core or log data. J. Sed. Petrol., 58, p 820-829.

Nesbitt, H.W., Young, G.M., 1982. Early Proterozoic climates and plate motions inferred from major element chemistry of lutites. Nature, 299: P715-717.

Roaldest, E., 1978. Mineralogical and chemical changes during weathering, transportation and sedimentation in different environments with particular references to the distribution of Ytrium and lanthanide elements. Ph.D. Thesis, Geol. Inst., Univ. of Oslo, Norway.

Said, R., 1962. The Geology of Egypt. Elsevier Publishing Company. Amsterdam – New York.

Salem, S.M., El-Gammal, E.A., Soliman, N.M., 2013. Morphostructural record of iron deposits in paleosols, cretaceous Nubia Sandstone of Lake Naser basin, Egypt, Western Desert, Egypt. The Egyptian Journal of Remote Sensing and Space Sciences. 16, p 71–82.

Tanner, L.H., Khalifa, M.A., 2009. Origin of ferricretes in fluvial-marine deposits of the Lower Cenomanian Bahariya Formation, Bahariya Oasis, Western Desert, Egypt. Journal of African Earth Sciences, 56, 179-189.